

Article

Technological Aspects of a Reparation of the Leading Edge of Helicopter Main Rotor Blades in Field Conditions

Michał Sałaciński ^{1,*}, Krzysztof Puchała ², Andrzej Leski ³ , Elżbieta Szymczyk ², Volodymyr Hutsaylyuk ² , Arkadiusz Bednarz ⁴ , Piotr Synaszko ¹, Rafał Kożera ⁵, Klaudia Olkowicz ¹  and Dominik Głowacki ⁶ 

¹ Air Force Institute of Technology, Airworthiness Division, 01-494 Warsaw, Poland; piotr.synaszko@itwl.pl (P.S.); klaudia.olkowicz@itwl.pl (K.O.)

² Faculty of Mechanical Engineering, Military University of Technology, 00-908 Warsaw, Poland; krzysztof.puchala@wat.edu.pl (K.P.); elzbieta.szymczyk@wat.edu.pl (E.S.); volodymyr.hutsaylyuk@wat.edu.pl (V.H.)

³ Łukasiewicz—Institute of Aviation, 02-256 Warsaw, Poland; andrzej.leski@ilot.lukasiewicz.gov.pl

⁴ Faculty of Mechanical Engineering and Aeronautics, Rzeszów University of Technology, 35-959 Rzeszow, Poland; abednarz@prz.edu.pl

⁵ Faculty of Materials Science and Engineering, Warsaw University of Technology, 02-507 Warsaw, Poland; rafal.kożera@pw.edu.pl

⁶ Faculty of Power and Aeronautical Engineering, Warsaw University of Technology, 00-665 Warsaw, Poland; dominik.glowacki@pw.edu.pl

* Correspondence: michal.salacinski@itwl.pl



Citation: Sałaciński, M.; Puchała, K.; Leski, A.; Szymczyk, E.; Hutsaylyuk, V.; Bednarz, A.; Synaszko, P.; Kożera, R.; Olkowicz, K.; Głowacki, D.

Technological Aspects of a Reparation of the Leading Edge of Helicopter Main Rotor Blades in Field Conditions. *Appl. Sci.* **2022**, *12*, 4249. <https://doi.org/10.3390/app12094249>

Academic Editors: Junwon Seo and Jong Wan Hu

Received: 18 March 2022

Accepted: 21 April 2022

Published: 22 April 2022

Publisher's Note: MDPI stays neutral with regard to jurisdictional claims in published maps and institutional affiliations.



Copyright: © 2022 by the authors. Licensee MDPI, Basel, Switzerland. This article is an open access article distributed under the terms and conditions of the Creative Commons Attribution (CC BY) license (<https://creativecommons.org/licenses/by/4.0/>).

Abstract: The Polish Air Force operates more than one hundred helicopters of the Mi family (manufactured by Mil Helicopters), equipped with metal main rotor blades. The main rotor blades are among the most stressed components of these structures. For this reason, they are subject to more frequent inspections during operation than other components. One type of damage detected during inspections is the local disbonding of fragments of the anti-erosion layer from the leading edge. This harmless-looking damage is very dangerous, since it quickly leads to the complete detachment of the layer. The leading edge, unprotected by the metal cover, erodes rapidly. The detached layer, when thrown away at high speed, endangers other parts of the helicopter, such as the tail rotor, and may cause damage to other helicopters if flying in formation. The technology supplied by the manufacturer to date has not encompassed the field repair of this type of damage. Therefore, efforts were made to develop repair technology for rapid repairs of blades in field conditions during missions of the Task Force White Eagle in Afghanistan. This article presents the concept of repair technology feasible in field conditions and presents the results of post-repair edge tests. Test results to identify the materials used in the construction of the trailing edge are also presented. The results of materials testing facilitated the development of technological processes, and, in the future, will aid the selection of a substitute bonding paste system with similar parameters that are essential for repairs.

Keywords: bonding; composite repair; aviation; rotor blades; helicopter

1. Introduction

While the rotor blades of Mi helicopters differ in profile and dimensions, their general design is similar for every type of helicopter (Figure 1) used by the Polish Armed Forces. The aluminum alloy spar is the rotor blade component responsible for transferring the main loads. The leading edge of the blade is equipped with an electric anti-icing device. A rubber cover and metal shield protect the electric anti-icing device. The trailing section is composed of a honeycomb metal sandwich structure. The trailing sections are bonded to the spar.

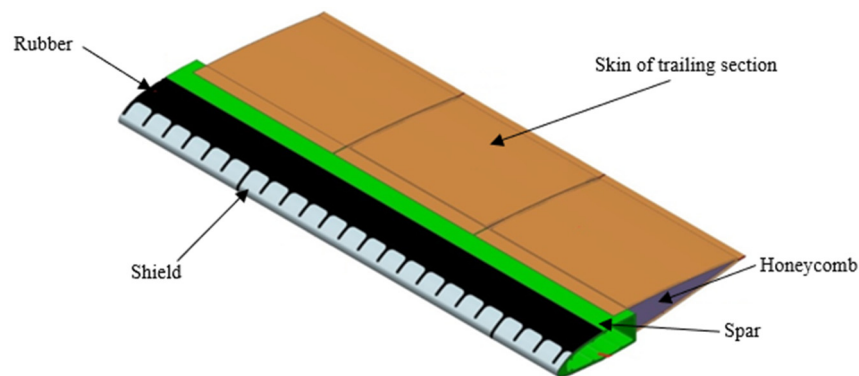


Figure 1. Structural baseline model of a Mi helicopter rotor blade.

During maintenance work on the main rotor blades, damage is detected in the form of a piece of the metal shield peeling off the leading edge (Figure 2). The detection of the damage makes it necessary to decide whether to repair the blade or to withdraw it from use.

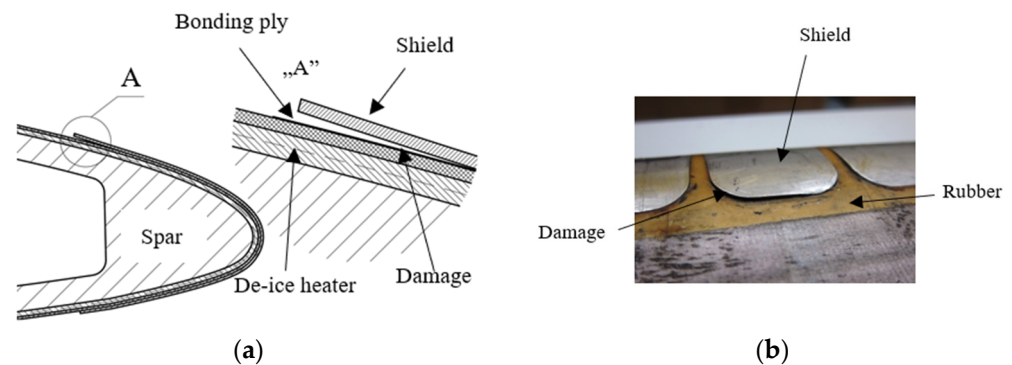


Figure 2. Damage to the leading edge—debonding shield from the leading edge: (a) Diagram; (b) Damage to a Mi-2 helicopter rotor blade (series 22-2700-3000).

The lack of repair technology for this type of damage can lead to the interruption of operational activities during military missions. Therefore, research was undertaken to develop a repair technology to quickly return the blades to service.

The high progressive velocity of the leading edge of the main rotor blade causes it to flap around at high speed. Dust, droplets of water, and ice in the air hit the leading edge at speeds of up to 200 m/s. Therefore, a metal shield protects the leading edge. The loss of the shield can cause damage to the blade. Local peeling quickly leads to the complete detachment of the shield. The leading edge unprotected by the metal cap is then rapidly eroded.

The available scientific publications on leading edges mainly focus on composite structures. Repairs of main rotors concern damage in the form of delamination or puncture [1]. Bonded joints are common in aerospace technology [2]. The problem of the erosion of unprotected metal shield blades of helicopter and wind turbine rotors composed of composite material was well illustrated in [3]. Repairs of damage to this type of blade are presented in publications [4,5]. The repair in both cases consists of the removal of the damaged composite layers and reconstructing the structure from new composite layers. Depending on the blade manufacturing technology, repair is performed with the use of wet or prepreg technology.

No publications were found on damage formation and the repair of shields debonding from the leading edge. Therefore, during the research presented in this paper, use was made of publications on bonding ply, surface preparation for bonding metals and rubber, and thermo-physical research on polymeric materials.

With respect to technological development, useful information was obtained from websites on helicopter blade repairs [6,7], which presented repair techniques for other typical damage to metal blades.

In addition, experience gained during other studies related to repairs to the metal blades of main rotors [8] was used. The phenomenon of the negative effects of temperature on polymeric materials was also addressed.

The aim of the paper is to present the validation/qualification of a developed repair technology for the leading edge of main helicopter rotor blades in field conditions.

2. Causes of Damage to and Conditions of Use of Main Helicopter Blades

The analysis of helicopter documentation (internal materials of the Polish Air Force) revealed that damage (Figure 2) is most frequently found on the blades of helicopters flown aggressively during real military missions. Damage is particularly common during missions such as cargo transport, maritime search and rescue missions, and assault operations. Damage is less frequently detected on helicopters used for training and routine flights. Damage of this type is only very rarely detected on blades with a short service history. It is therefore concluded that the damage is influenced by the intensity of operation, which consists of mechanical loads and environmental conditions.

2.1. Mechanical Loads

The main rotor blades are one of the most stressed components of a helicopter. Even when the helicopter is in a static condition, the blades are subjected to high static loads due to their mass. However, during flight, the blades are subjected to dynamically varying complex loading conditions, resulting in longitudinal and torsional loading (Figure 3).

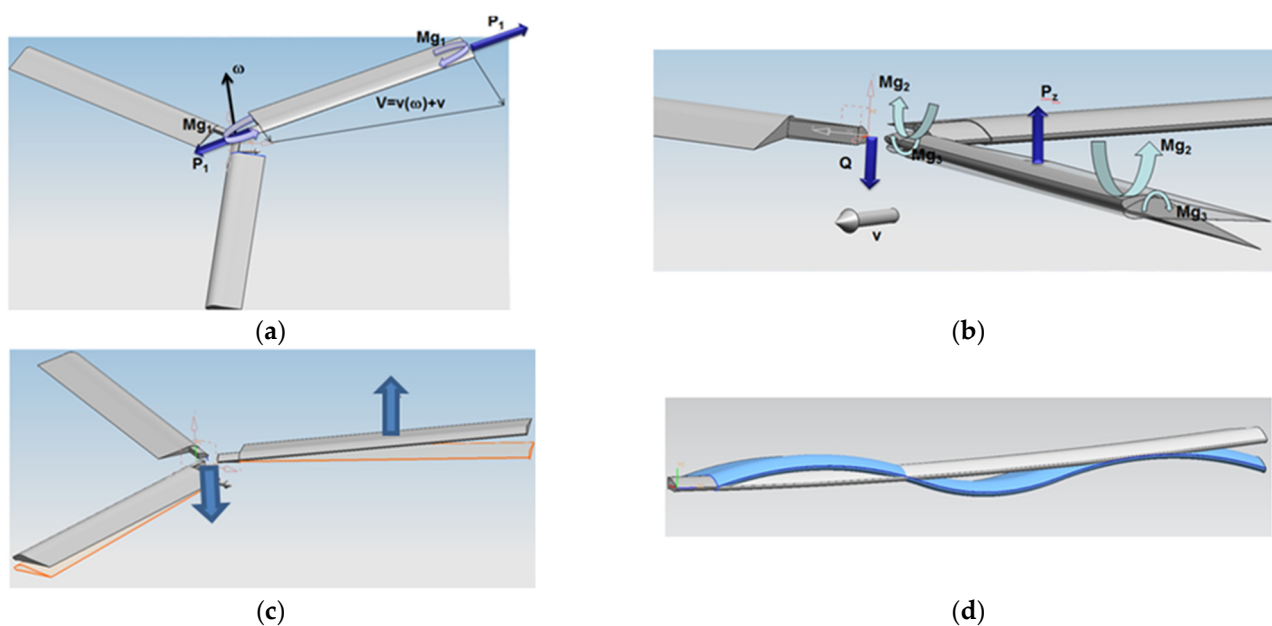


Figure 3. Diagram of loads on helicopter rotor blades: (a) Tensile force—centrifugal P_1 , moment bending the blade in the direction of flow Mg_1 ; (b) Lift force P_z , bending moment related to the induced drag— Mg_2 ; aerodynamic moment Mg_3 ; (c) Loads related to the change in position of the blades during flight; (d) One vibration mode.

The numerical calculations presented in [9–11] show that, due to the deformation of the blade, a stress concentration occurs in the bonding ply between the shield and the rubber. At the maximum deflection of the spar, the stress in the bonding ply approaches the maximum permitted stress [12]. Therefore, it can be assumed that stress concentration may cause damage.

2.2. Environmental Factors

Temperature is one of the environmental factors affecting the durability of an adhesive bond [13]. Even small changes in the temperature of bonded elements with different coefficients of thermal expansion can cause microcracking in the bonding ply [14], accelerate the diffusion of contaminants, and accelerate creep [15]. Thermo-physical transformations occurring in polymer adhesives are equally dangerous for bonded structures. Thermo-physical transformations occur at particular temperatures and change the mechanical properties of the material [16,17].

The manufacturer has not set up a strictly defined operating temperature range for Mi helicopters.

The Certification Specifications for Large Rotorcraft CS-29 [18] do not explicitly define the maximum operating temperature of main rotor blades. However, since temperature can play a part in the occurrence of damage in factory-made adhesive joints both during operation and during the process of repair of damaged parts, it was decided to take temperature into account in the testing of bonds during the development of repair technology. The range of operating temperature for the research was adopted based on the helicopter flight profile in the Polish Armed Forces (flight altitude and places of operation—environment) and the results of temperature measurements of the leading edge anti-icing device heating system.

The ceiling for Mi helicopters is 4.5 km above sea level, which, according to the ISA [19], translates into a minimum temperature of approx. $-20\text{ }^{\circ}\text{C}$. The locations where the Polish Armed Forces helicopters fly is classified information, but the users of the helicopters stated that they operate within the ambient temperature range of $-40 \div +50\text{ }^{\circ}\text{C}$.

Publication [20] presents the results of thermal imaging tests of the Mi-8 helicopter rotor blade with the leading edge anti-icing device system activated. According to the measurements, the anti-icing device system can heat the leading edge up to $40\text{ }^{\circ}\text{C}$. This is, therefore, lower than the maximum operating temperature resulting from environmental effects.

Therefore, it can be assumed that the operating temperature of the blades is within the range of $-40 \div +50\text{ }^{\circ}\text{C}$.

The second environmental factor that particularly negatively impacts adhesive joints is moisture, as was shown by the research presented in [21]. As in the case of temperature, the manufacturer did not indicate the permissible level of ambient humidity during the operation and storage of the blades. Therefore, the Certification Specifications for Large Rotorcraft CS-29 were used [19]. Subsection CS29.45 states that the maximum ambient relative humidity during operation is 80%. Based on the aforementioned study [21], it is surmised that prolonged exposure to 80% humidity can significantly contribute to adhesive bond failures. Therefore, the effect of humidity on adhesive bonds should be considered in qualification tests.

3. Materials

The blade performance records held by the Polish Air Force do not contain full detailed information about the materials used in the design of main rotor blades. In order to obtain the relevant properties of the materials used in the leading edge, which are required for the purpose of formulating an appropriate repair process, it was decided to conduct a study to identify the necessary data.

With regard to a metal shield, an important piece of information when designing the repair process is the composition of the alloy out of which it is made. With this information, an appropriate surface preparation method can be developed. On the other hand, with polymer materials—rubber and adhesives—the thermo-physical properties constitute vital data. The thermo-physical properties will determine both the properties of the replacement bonding ply and the parameters of the thermal processes during repair.

Helicopter blades can stay in service for seven years from the date of manufacture. Samples for the study were taken from the blade just after it was taken out of service.

Therefore, it was assumed that the materials had not degraded and the properties of the materials out of which they were produced did not differ from blades in service.

3.1. Shield Material

The chemical composition of the metal shield was analyzed using an Olympus Delta Professional handheld XRF X-ray spectrometer. A sample taken from the blade shield (Figure 4), was tested at three randomly selected positions. The metal was identified as titanium alloy (Table 1).



Figure 4. Sample of a shield for the XRF identification tests.

Table 1. XRF-identified composition of the sheath material.

Test 1	Test 2	Test 3	Average	Standard Deviation
Ti	Ti	Ti	Ti	Ti
96.60%	97.74%	97.55%	97.96%	0.60%
Mn	Mn	Mn	Mn	Mn
1.29%	1.06%	1.15%	1.16%	0.11%
Al	Al	Al	Al	Al
-	1.12%	1.18%	0.76%	0.04%
Fe	Fe	Fe	Fe	Fe
-	0.07%	0.07%	0.05%	0%
Si	Si	Si	Si	Si
0.11%	-	0.05%	0.13%	0.05%

3.2. Polymer Materials

Leading edge repair technology involves the local heating of the structure, both for the complete detachment of the shield from the rubber, which is necessary to prepare the bonding surface, and for the subsequent post-curing of the new epoxy resin-based adhesive. Both processes take place at temperatures as high as 110 °C. Consequently, it is essential for the rubber and adhesive that the polymer components of the blade remain thermally stable after the annealing operations performed during the repair process. Thermal stability is a general term used to describe the changes (or lack of changes) in material properties as a function of temperature [16].

A differential scanning calorimetry (DSC) study was conducted to verify the behavior of the leading edge rubber and the bonding ply that connects the rubber to the shield.

The study of the thermo-physical properties was carried out on one sample of each material. According to [20], one sample of a given material is sufficient to estimate the properties associated with thermo-physical transformations.

The bonding ply sample was taken from the rubber surface after the shield has detached from the rubber, as per Figure 5a. The rubber sample was cut out from the top of the leading edge, as shown in Figure 5b. The samples were cut to fit a standard 146.33 mg aluminum DSC crucible. The bonding ply sample weight was 75.82 mg and the rubber sample weight was 92.45 mg.

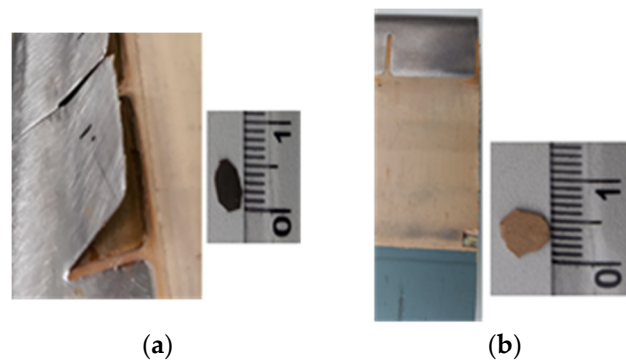


Figure 5. Sampling site and samples for DSC testing: (a) Bonding ply; (b) Rubber.

DSC was performed using a TA Instrument DSC Q1000. The samples were tested in the temperature range of $-90 \div 110$ °C.

The lower limit of -90 °C was adopted for DSC testing to check whether the materials crystallize—enter a brittle state—which is unacceptable for materials used in aviation. This study was based on the conclusion of [22,23], where the author of the work showed that transformations at temperatures below the aircraft operating limit can impinge on the material properties in the operating range of the tested material, despite the presence of a reversible phase transition. The DSC test included four thermal cycles carried out consecutively on one specimen:

1. Cycle 20 °C \rightarrow -90 °C \rightarrow 50 °C \rightarrow 20 °C—fly simulation I;
2. Cycle 20 °C \rightarrow -90 °C \rightarrow 50 °C \rightarrow 20 °C—fly simulation II;
3. Cycle 20 °C \rightarrow 110 °C \rightarrow 20 °C—process repair simulation;
4. Cycle 20 °C \rightarrow -90 °C \rightarrow 50 °C \rightarrow 20 °C cycle—fly simulation III.

The rate of temperature change for each cycle was 5 °C/min. The sample was in a helium atmosphere during the test. The DSC results are shown in Figure 6.

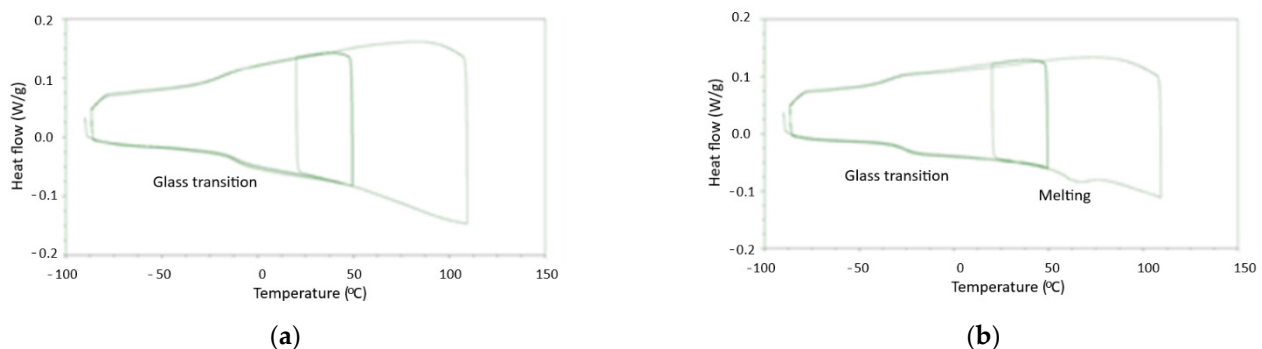


Figure 6. Results of the DSC tests of the rotor blade edge components: (a) Bonding ply; (b) Rubber.

The glass transition temperatures were determined for both the rubber and bonding ply. They were -26 °C for rubber and -11 °C for bonding ply. Moreover, the DSC curves for the rubber showed an endothermic peak at 65 °C with low enthalpy. It can be supposed that this peak is related to the moisture content of the rubber. For bonding ply in the temperature range of -20 °C to 110 °C, no permanent transformations were observed due to the action of both the simulated temperature changes alone during service and those resulting from the thermal cycle during curing. This indicates that both materials are thermally stable over the studied temperature range.

4. Repair Technology

The concept of the repair of the detachment of the shield fragment from the leading edge of the main rotor blade consists of the separation and bending of the shield fragment

from the rubber, proper drying and preparation of the surface for bonding (mechanical and chemical), application of properly selected adhesive, pressing the shield fragment to the edge, and conducting the appropriate thermal cycle of curing the adhesive. The process is shown step-by-step in Figure 7.

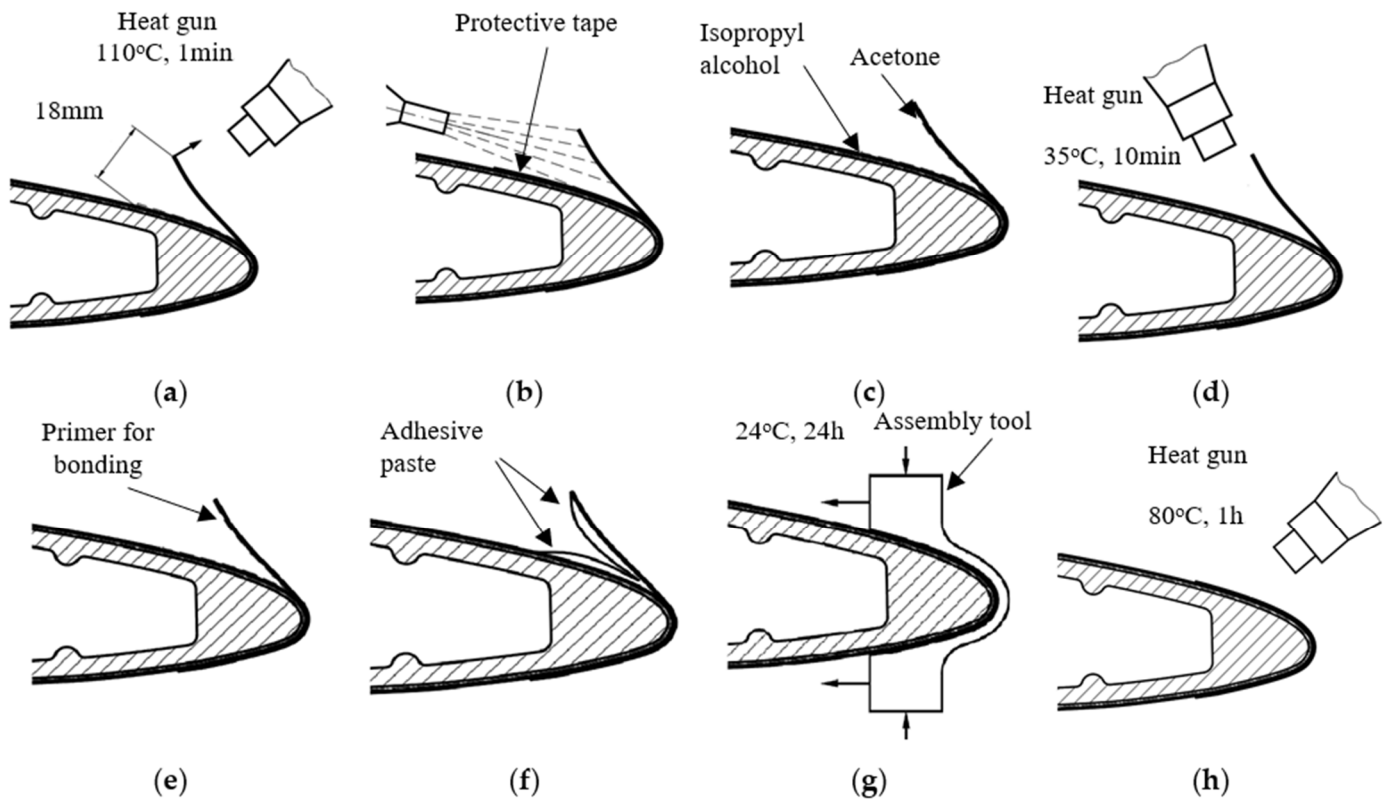


Figure 7. Technological process of repairing the leading edge of a rotor blade: (a) Separation of the damaged piece of shield from the rubber; (b) Sandblasting; (c) Cleaning; (d) Drying; (e) Applying a primer; (f) Applying adhesive paste; (g) Curing; (h) Post-curing.

In order to properly prepare the surface for bonding, the faulty shield must be separated from the rubber (Figure 7a). Based on the DSC analysis (Figure 6) and a number of tests, it was found that heating the shield to 110 °C softened the bonding paste so that it could be peeled off with a medical wooden spatula.

It was tentatively assumed that an epoxy resin-based adhesive system, containing fillers to increase the viscosity of the bonding paste, would be used for bonding the shield during repair.

When bonding, especially using epoxy resin-based systems, surface preparation is one of the most important parts of the bonding process. According to [24], a titanium surface before bonding can be prepared using various mechanical, chemical, and electrochemical methods. However, the most important issue is to create appropriate roughness on the prepared surface.

In [24], an illustrative classification of bond strength and durability, from poor to excellent, was presented. Degreasing and then scrubbing with sandpaper affords irregular macroporosity to the surface [25]. According to the classification presented, roughening with sandpaper produces “poor strength” and “poor durability”. In contrast, sandblasting yields uniform macro roughness, which translates to “increased strength” and “adequate durability” of the joint. “Excellent properties” are achieved by chromic acid anodizing [26] and other chemical treatments, such as sol-gel [9,21,27] or modified phosphate fluoride processes [28]. These methods produce a microporous surface coated with titanium compounds that is supersaturated with adhesive. Unfortunately, it is not feasible to use these

methods in field workshop conditions. These methods require the use of toxic and chemically aggressive reagents (chromic acid VI) in appropriate proportions, and specialized apparatus in the case of anodizing. The use of aggressive chemicals, which, in an uncontrolled manner would penetrate the gaps created by a partially detached shield, could lead to the degradation of components during subsequent operation. In addition, in the case of selected fragments of partially detached shield, the use of electrochemical methods is technically very difficult.

Therefore, the decision was made to treat the titanium surface in a way that is feasible in field workshop conditions, consisting of surface degreasing and sandblasting (Figure 7b). Sandblasting using a 6 mm-diameter nozzle, 0.4 mm-grade corundum sand, and 10 bar working pressure at 2 m³/min, resulted in a roughness of Ra = 1.05 µm. Before this operation, the rubber was protected by isolation tape, which was removed after sandblasting.

The surface after sandblasting should be washed with acetone to remove sand dust and oil residues (Figure 7c). Despite the use of oil separators in the pressure supply system of the sandblasting gun, there is a risk that trace amounts of oil mist from the compressor lubrication system may be present in the compressed air.

The pieces of old bonding ply remain on the rubber after the separation of the metal shield from the rubber. There are two ways to remove them: mechanically or chemically. The mechanical attempts with sandpaper caused damage to the rubber. Therefore, the chemical method was applied. According to the manual [12] for the cleaning of the rubber on the leading edge, gasoline or isopropyl alcohol can be used. The tests showed that gasoline was not effective for the removal of the old bonding ply residue, so isopropyl alcohol was chosen. Cleaning was conducted by wiping the rubber surface with a cotton cloth slightly dampened in isopropyl alcohol. Isopropyl alcohol evaporates quickly after cleaning, so it does not pose a further threat to the rubber and to the new joint.

The development of the surface preparation method was laboratory-tested using the water-break test method, using distilled water in accordance with [29–31]. During the repair of an actual main rotor blade, this test will not be possible because it would significantly complicate the bonding process—it is difficult to dry the water in the slots, as well as check that the drying was conducted correctly. It was assumed that surface preparation and cleaning must be performed according to the developed method. This guarantees a properly prepared surface for bonding.

The surfaces have to be dried by a heat gun (Figure 7d) after chemical cleaning (shield with acetone and rubber with isopropyl alcohol). Although the fact that the solvents used evaporated easily, drying requires quite a long time to remove them from porous structures—sandblasted metal and rubber. Based on experience, 10 min at 35 °C was assumed to be sufficient. After the cooling of the surfaces, the primer is applied by a brush (Figure 7e). The primer is cured in ambient conditions for 8 h [32,33].

Contrary to appearance, the application of adhesive paste is a complicated process. The paste applied to the target surfaces should be as shown in Figure 7f, with the thickest layer being about 3 mm. In this way, when the elements are pressed together, the excess adhesive paste will flow out, leaving an even layer between them. Applying the paste in the same thickness on the entire surface (without the characteristic bulges) or leaving a layer containing air bubbles will cause the adhesive to be uneven when pressed, or air bubbles will form in the center (Figure 8).

The shield is composed of a titanium alloy characterized by a high modulus of elasticity. Therefore, clamping the shield during bonding requires significant force evenly distributed over the surface of the shield (Figure 7g). In order to achieve this, an assembly tool was designed and manufactured to press the shield properly against the edge, allowing the blade profile to be reproduced (Figure 9).

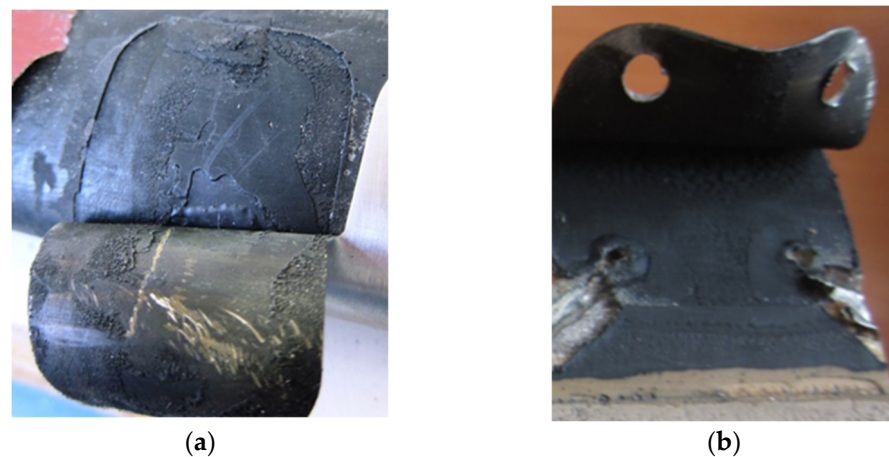


Figure 8. Fracture surfaces of bonding layers: (a) Bonding ply with voids—wet adhesive paste was not properly applied; (b) Bonding ply without voids—wet adhesive paste was correctly applied.

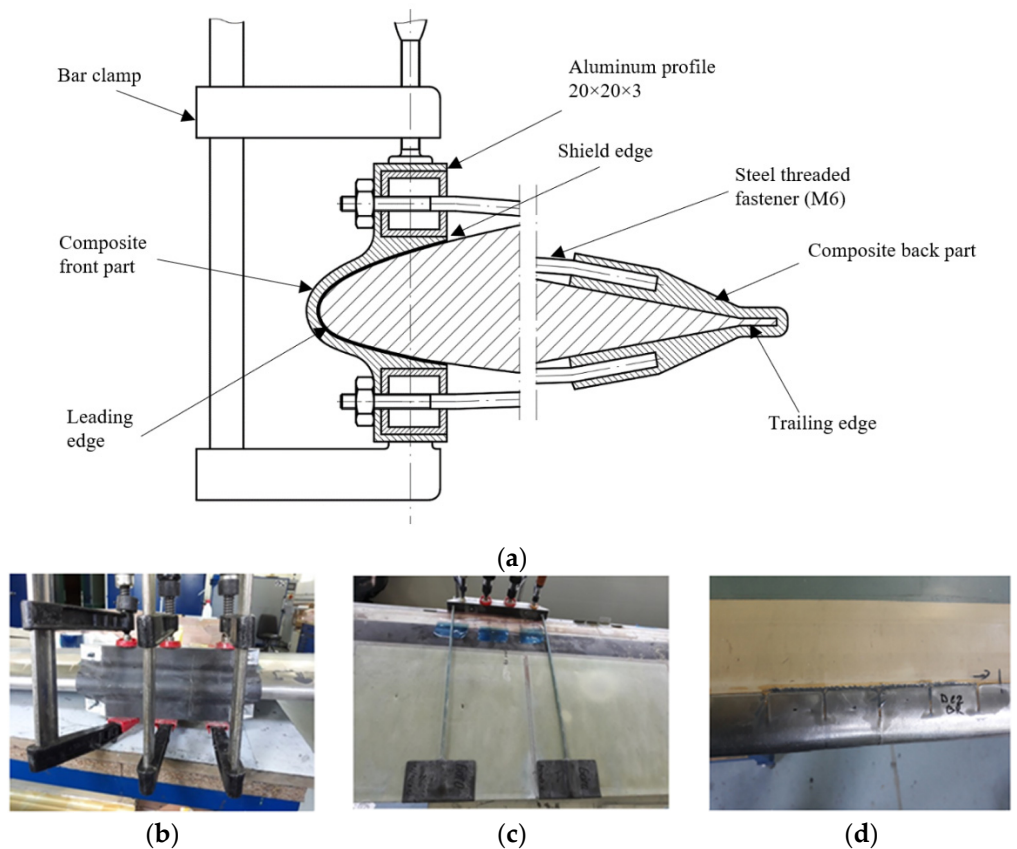


Figure 9. Bonding process: (a) Assembly tool—scheme; (b) Assembly tool—front; (c) Assembly tool—top/back; (d) Leading edge after repair.

The composite back parts of the assembly tool (Figure 9a) were installed on the trailing edge of the blade first. Next, the bonded shield was compressed to the leading edge using the composite front part of the assembly tool by hand after applying adhesive paste to the bonded surfaces of the leading edge under repair. Then, the front part of the assembly tool was joined to the back part of the assembly tool using a fastener (M6). Therefore, the shield was pressed to the leading edge. In order to additionally pressed the shield to the top and bottom of the leading edge, bar clamps were installed as the last step. The excess adhesive paste squeezed out was removed by a wooden spatula.

The last step was the curing process—hardening (Figure 7g) and post-curing process—improvement properties (Figure 7h). For typical epoxy adhesive paste, the curing temperature is 24 °C for 24 h and the post-curing temperature is 80 °C for 1 h. Epoxides are cross-linked polymers. The first crosslinking step occurs during curing through the action of the curing agent. The temperature treatment causes the bonds to strengthen, which translates into increased strength and durability of the bonding ply. The repaired leading edge area is shown in Figure 9d.

5. Repair Qualification Study

Two 3M epoxy adhesive pastes and three methods of metal surface preparation were selected based on the identification of the materials used in the construction of the rotor blade and the data sheets of materials intended for aviation purposes.

The adhesive pastes were DP490 [34] and 2216B/A [35]. The methods of metal surface preparation were as follows: without a primer; with the use of Rafil chemically resistant epoxy primer paint [32], and Cytec primer BR-127 [33].

According to the data sheets, the selected adhesive pastes can be used for bonding metals and rubber. They are characterized by high strength and flexibility, which is crucial in the case of bonding rubber to metal. DCS tests were not included in the qualification study because the selected materials are approved for use in aviation.

5.1. First Stage—Preliminary Selection of Bonding

The first and simplest selection of a bonding system consists of verification of the nature of the damage (which components of the bonding layer were damaged) during the static tearing off of the shield (Figure 10). It was assumed that further, more advanced testing is feasible only in those bonding systems with the decohesive fracture type in the bonding layer or rubber. It would indicate that the surface preparation and primer were correctly selected and that the maximum transferring load was via the bonding layer or rubber.



Figure 10. Scheme of tearing off the shield during preliminary tests: (a) crack initiation with a chisel, (b) tearing off the shield with universal pliers.

The test results were as follows:

1. Bonding 2216B/A—deadhesive fracture surfaces between the metal and bonding layer;
2. Bonding 2216B/A + Rafil primer—decohesive fracture surfaces of the primer;
3. Bonding 2216B/A + BR-127 primer—decohesive fracture surfaces of the bonding layer;
4. Bonding DP490—no damage to the bonding layer, decohesive fracture surface of the rubber;
5. Bonding DP490 + Rafil primer—decohesive fracture surfaces of the primer;
6. Bonding DP490 + BR-127 primer—deadhesive fracture surfaces between the metal and bonding layer.

According to the above criterion, only the following systems were further tested:

- Bonding 2216B/A + BR-127 primer;
- Bonding DP490.

5.2. Second Stage—Strength Test of the Bonding Systems

A strength test of the bonding system between the metal shield and rubber was carried out by two methods:

1. Shear strength test;
2. Comparative study of the tearing off the shield from the fragment of the rotor blade. During the test, the originally manufactured bonding system was compared to the bonding systems produced according to the proposed technology.

The mechanical properties of materials depend on their temperature and moisture content. At higher temperatures and humidities, moisture may be absorbed, which may lead to the material swelling [36,37]. In a cold climate, the influence of water and temperature on materials is associated with the freeze–thaw cycle [38,39]. Therefore, in order to study the influence of the operating/usage environment's parameters on the performed repair, some of the samples were aged in a climatic chamber.

The aging program was developed on the basis of information on the operating conditions of aircraft and military equipment, military regulations, and International Standard Atmosphere (ISA) [39–48]. During the program, the samples were aged in four cycles for a total of 30 h and 45 min. One cycle of exposure in a climatic chamber consisted of four segments: increase in temperature and humidity; maintaining temperatures at 50 °C and relative humidity at 80% for 3 h; decrease in temperature and humidity; and maintaining temperatures at −40 °C for 3 h. The cycle was repeated four times (Figure 11). The aging of the samples was performed using a DM 340 SR climatic chamber (Angelantoni Test Technologies).

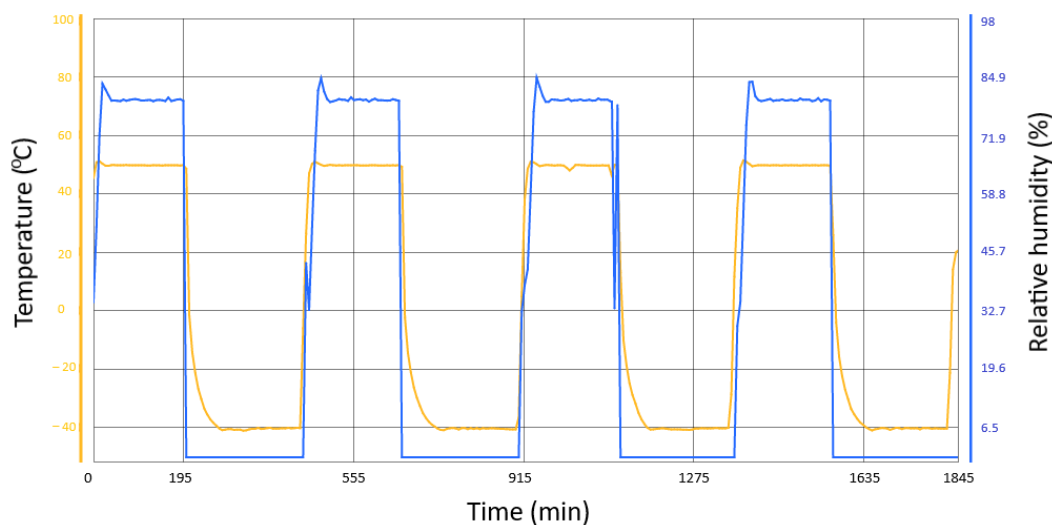


Figure 11. Exposure conditions of samples in a climatic chamber during the aging program.

5.2.1. Shear Strength Test

It was assumed that, if the strength is greater than the value of the allowable stress in the bonding or if the fracture of the rubber is decohesive in nature, the adhesive system will be considered correct. The strength criterion results from the fact that the tests carried out during the development of this technology concern the connection of a fragment of the rotor blade covered with a layer of rubber and a sheet composed of Ti-6Al-4V alloy [49], the properties of which are similar to those of the alloy of the shield (Figure 12). The allowable stress value of the bonding layer is $\tau^{\text{ult}} = 3.92$ MPa, which was taken from the repair instructions developed by the rotor blade manufacturer and published by the Polish Air Force [12]. The description of the tests contained in the instructions pointed out that the value of the allowable stress in the bonding layer $\tau^{\text{ult}} = 3.92$ MPa obtained during laboratory tests was equivalent to that in single-lap joint tests [50], and it concerned only the strength of the bonding layer. Therefore, the tests presented in this article and the

test by which the limit value was obtained differ from one another. Focusing only on one criterion, consisting of comparing the obtained results and the limit values, was considered insufficient. A fragment of the sample with rubber was taken from the lower part of the leading edge of the rotor blade (Figure 13).

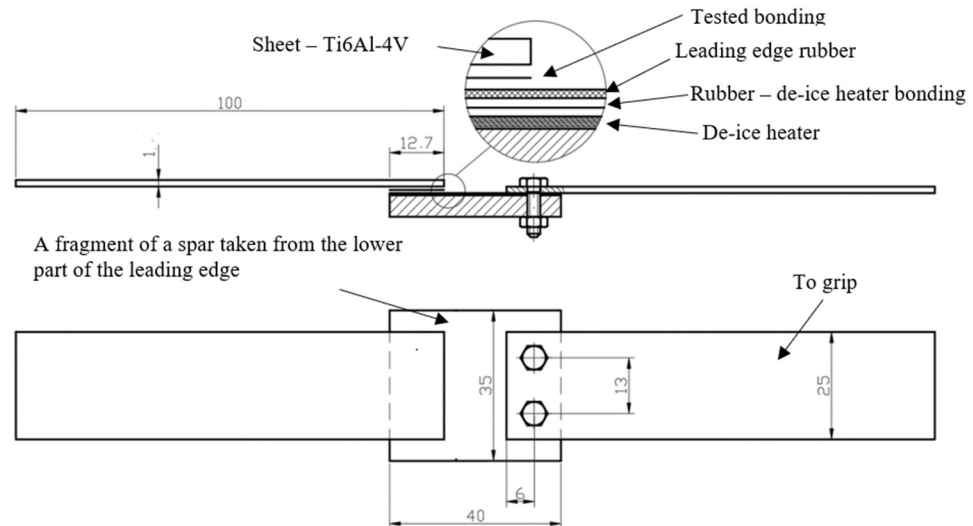


Figure 12. Scheme of the sample for shear strength tests of the leading edge shield and rubber bonding.

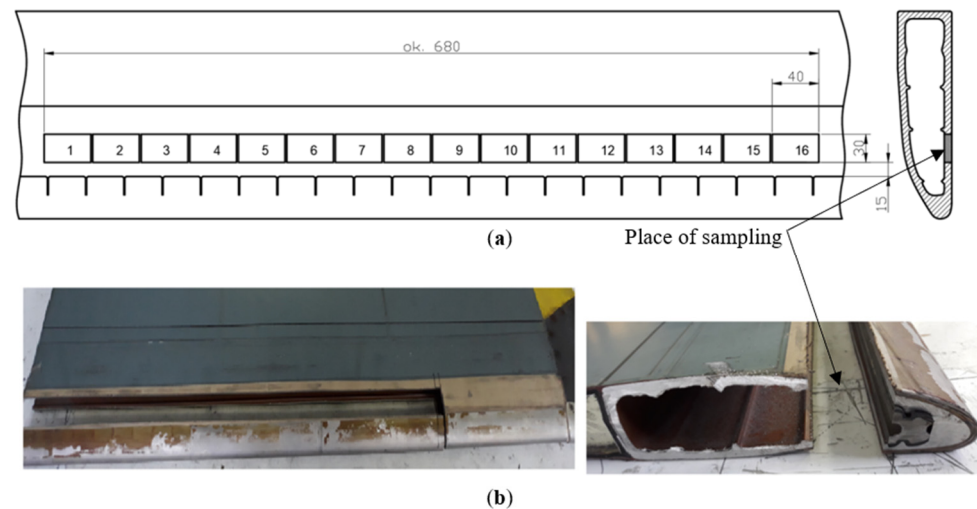


Figure 13. Place from where the spar fragments were extracted: (a) scheme of spar; (b) Mi-8 rotor blades after collecting samples.

The surfaces for the bonding process were treated according to the proposed repair technology. The limited possibilities of obtaining spar fragments resulted in only eight samples being produced for each variant:

1. Bonding 2216B/A + BR-127 primer;
2. Bonding DP490.

Four samples after aging and four samples without aging were strength-tested.

The shear strength test of bonding was carried out on an Instron Fatigue system. A constant speed of actuator movement equal to 2 mm/min was applied. Force was recorded as a function of displacement, on the basis of which the shear stresses were determined. The damage caused by the shearing of bonding 2216B/A + BR 127 primer after aging, was characterized by adhesive fracture surfaces between the bonding layer and rubber (Figure 14a). The rest of the samples were characterized by the cohesive fracture surface of the rubber (Figure 14b–d).

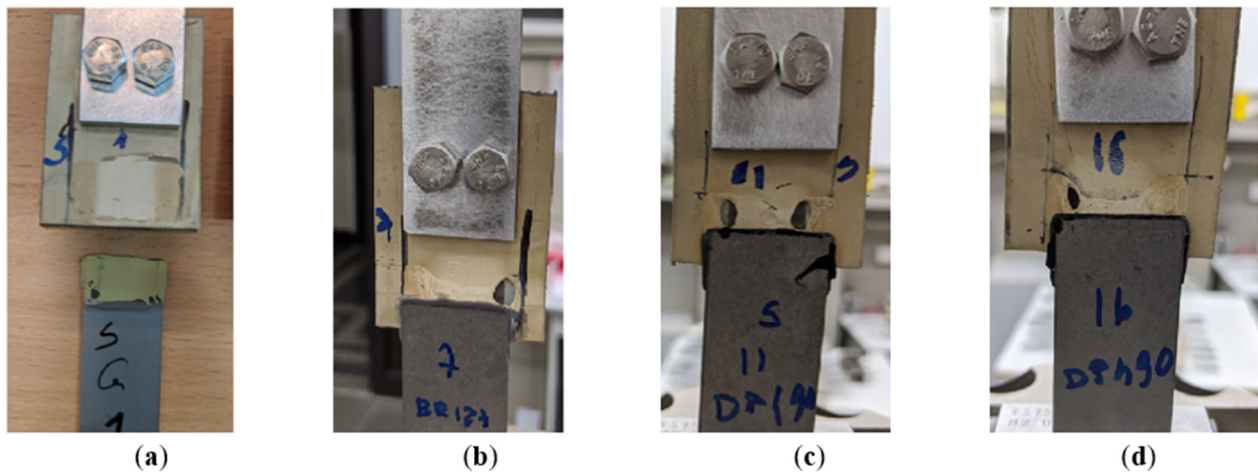


Figure 14. Characteristics of fractures during the shear strength test: (a) Bonding 2216B/A + BR-127 primer after aging; (b) Bonding 2216B/A + BR-127 primer without aging; (c) Bonding DP490 after aging, (d) bonding DP490 without aging.

The results of the bonding 2216B/A + BR primer samples without aging and after aging obtained during the shear strength test are given in Figure 15. In the case of the samples after aging, the spread of the results was considerable, and, for this reason, the average value and standard deviation were not calculated.

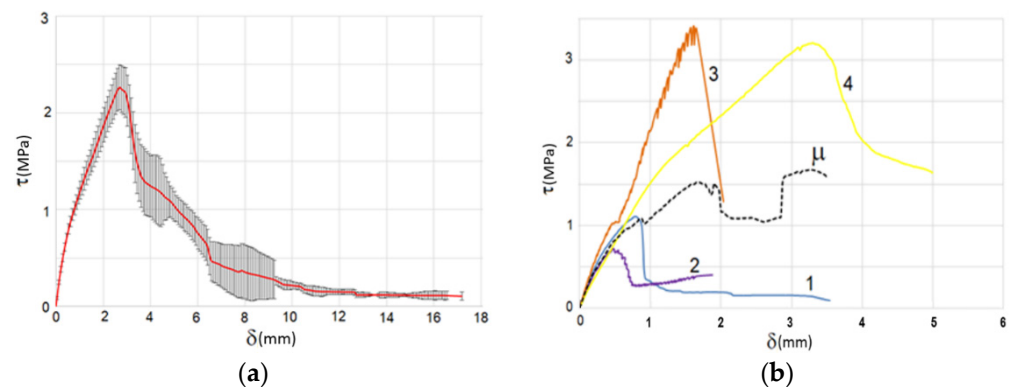


Figure 15. Results of the bonding 2216B/A + BR primer obtained during the shear strength test: (a) Samples without aging; (b) samples after aging.

The reason for the large discrepancy in the strength test results of the joint (Figure 15b) may be the degradation of the polymeric materials in the joint. Degradation is referred to as the partial disintegration of a polymer—not into low-molecular-weight products, but into fragments of high but lower molecular weight than the initial polymer. Factors initiating degradation may be physical or chemical interactions, such as radiation, temperature, or exposure to chemicals, including water [51–54].

The shear stresses of the joints of samples without aging were calculated. Despite the fact that the results were less than $\tau^{\text{ult}} = 3.92$ MPa, the rubber was damaged instead of the bonding. Therefore, it should be assumed that the strength condition was met. A very large dispersion of the results after the aging of the samples and adhesive fracture surfaces between the rubber and bonding layers testify to the high influence of the environmental conditions on bonding.

The average values of the shear stresses and standard deviation of the bonding DP490 samples are given in Figure 16. Despite the fact that the shear strength was less than $\tau^{\text{ult}} = 3.92$ MPa, the rubber was damaged instead of the bonding. Therefore, it should be assumed that the strength criteria were met for samples after aging and without aging. It

should be noted that the strength of the bonding after aging was lower in relation to the strength of the bonding without aging. Moreover, the standard deviation of the samples after aging was greater.

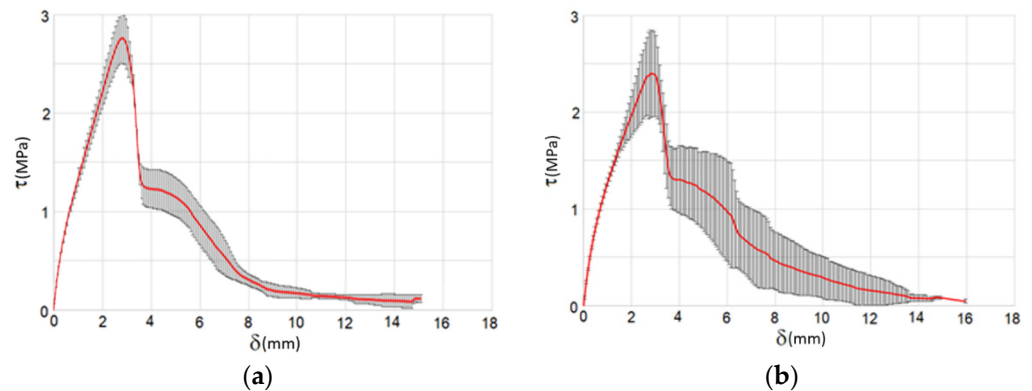


Figure 16. Results of the bonding DP490 obtained during the shear strength test: (a) samples without aging, (b) samples after aging.

Based on the research, it was found that the bonding 2216B/A + BR-127 primer could not be used to repair the leading edge. This was mainly due to the too large deviation of the strength test results for the samples after aging. Material with unstable properties should not be used in aviation. Therefore, it was decided to terminate the research with the use of this adhesive system.

5.2.2. Comparative Tests of the Tearing Off the Shield from the Leading Edge

The test consisted of a comparison of the tearing force F (Figure 17) of the shield parts with the factory bonding and the bonding created according to the proposed technology (Bonding DP490). The test was also carried out on an Instron Fatigue system. The constant speed of actuator movement equal to 2 mm/min was applied. Force was recorded as a function of displacement. Five samples from each series were tested. Distinctive fractures of bonding are given in Figure 18. All the fractures were cohesive; therefore, the rubber was damaged.

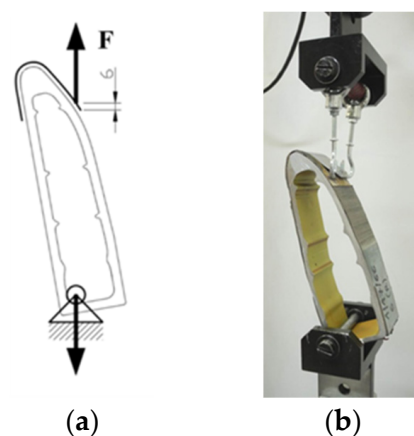


Figure 17. Comparative tests of the tearing off of the shield from the leading edge: (a) Scheme, (b) Sample on the test stand.

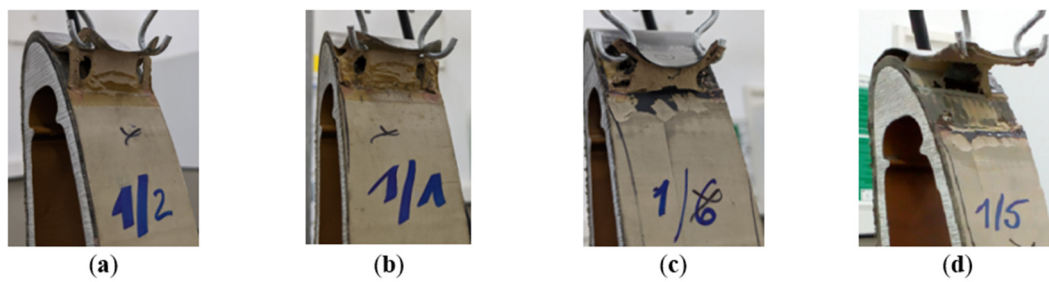


Figure 18. Characteristics of fractures during tests of the tearing off of the shield from the leading edge: (a) Factory bonding sample without aging, (b) Factory bonding sample after aging, (c) Bonding DP490 sample without aging, (d) Bonding DP490 sample after aging.

The results of test of the tearing off of the shield from the leading edge are given in Figure 19.

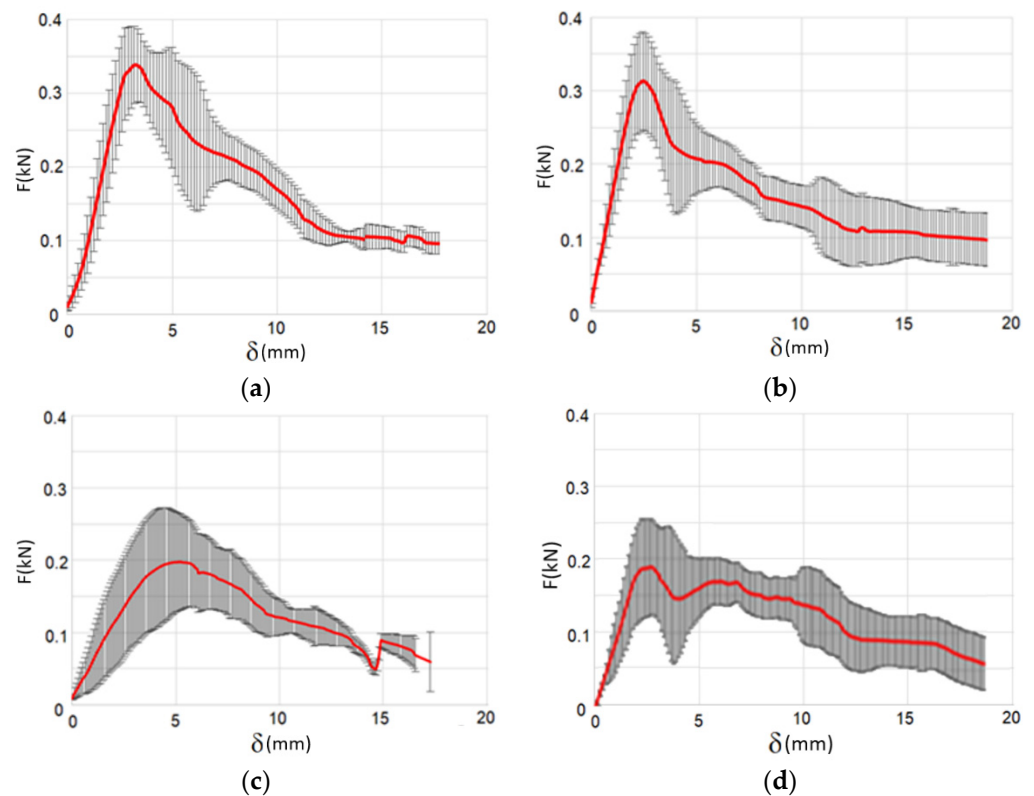


Figure 19. Results of the comparative tests of the tearing off of the shield from the leading edge: (a) Factory-bonded sample without aging; (b) Factory-bonded sample after aging; (c) DP490 bonding sample without aging; (d) DP490 bonding sample after aging.

The strength of the DP490 bonding was lower by about 30% in comparison to the factory bonding. The determined standard deviation indicated that the dispersion of the results was greater in the case of the DP490 bonding. The exposure in the climatic chamber did not affect the strength of the bond, both in the case of the factory bonding and the DP490 bonding.

The differences in strength between the factory-bonded samples and samples after the proposed repair technology may be due to the fact that, during preparation for repair, the shield must be folded back, and thus residual stresses are introduced. Due to these stresses, the tearing force is lower than that in the case of factory bonding.

The test samples were taken from a main rotor blade operated on a helicopter. Therefore, the factory bonding was exposed to actual atmospheric conditions. Similarly, the aged

DP490 bonded samples were exposed to variable climatic chamber conditions. In these cases, the maximum force occurred at a displacement of about 2.5 mm during the tearing off of the shield from the leading edge.

The maximum force occurred at a displacement of approximately 5 mm during the test of the bonding DP490 samples without aging.

It was assumed that the faster force increase was due to internal stresses in the bonding ply and at the rubber–bonding ply border as the result of aging processes under environmental conditions.

6. Checking the Condition of the Shield after Repair

The tap-test method was used to check the adhesive bond [55,56]. The test showed that the difference in sound frequency between the undamaged and damaged bonding ply was 780 Hz and the difference in amplitude was 16 dB. Such large differences in parameters allow assessing the condition of the bonded joints. The test was conducted with an environment noise level of about 40 dB (Figure 20).

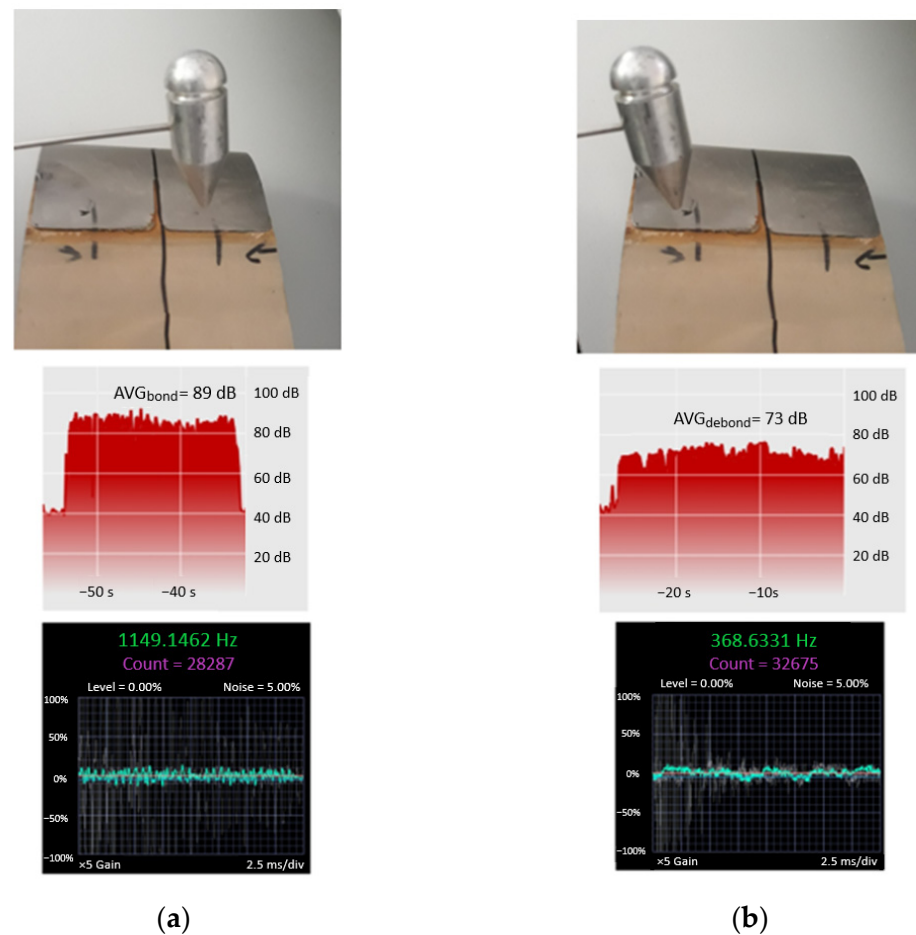


Figure 20. Tap-test of a reference sample with sound intensity and frequency measurement: (a) Shield bonded; (b) Shield disbonded.

The tap-test of the edge after repair was applied according to Figure 21 starting approximately 1 mm from the edge of the shield.

Tap-tests were carried out on the repaired structure (Figure 9d) as described above. The tests showed 100% adhesion over the entire area to be repaired—four sections of the shield. This means that the adhesive layer was evenly spread and the designed mounting tool applied the correct pressure.

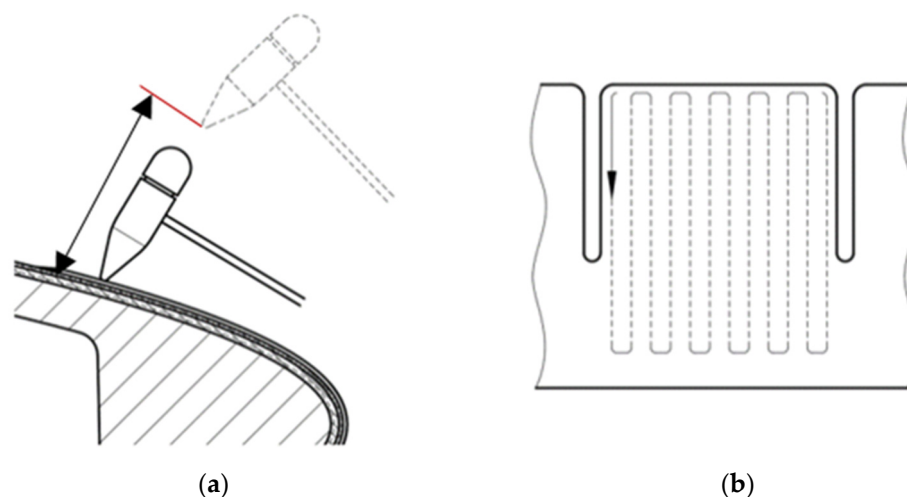


Figure 21. Non-destructive testing: (a) Method of tap-test with an inspection hammer; (b) Trajectory of the tap-test.

7. Conclusions

To date, the technology supplied by the manufacturer of Mi helicopter blades has not included instructions for the repair of leading edge deformations in field conditions. Therefore, a technology was developed and described in this paper, which presented the leading edge design of Mi helicopters. A number of factors may contribute to blade damage, as the frequency of damage is related to the intensity of operation. Based on an analysis of literature, operation, and technical documentation, the mechanical loads of blades were characterized and the environmental conditions affecting blades were determined: temperature range $-40 \div 50$ °C and maximum humidity of 80%. Due to the lack of data on the materials used in production, tests were carried out to identify the material properties relevant to the operation and repair technology. Spectroscopy was used to determine that a titanium alloy was used for the shield. This affected the selection of appropriate sandblasting parameters for surface treatment prior to bonding.

DCS analysis was performed to check the thermal stability of the polymer materials used on the leading edge. This information was useful in the development of the technological process related to detaching the damaged section of the leading edge. Knowledge of the thermo-physical properties was essential for initially selecting the bonding systems for further research.

Using the designed assembly device, a repair demonstrator and the samples for testing were produced.

The reference samples produced for non-destructive testing were used for the validation of the tap-test method as a service diagnostic method. The verification confirmed that the repair was carried out correctly.

The strength tests showed that the repaired bonded joint was 30% weaker in comparison to the factory-made joint.

Differences in strength between the factory bonding samples and samples after the proposed repair technology may be due to the residual stresses, introduced during the repair process. This phenomenon requires further research and will be studied in the future. The environmental impact on the strength properties of the repair was negligible.

The Polish Air Force approved the considered technology for supervised operation at the end of 2019. Within two years, the Air Force has not reported any problems with the repaired rotor blades.

Author Contributions: Conceptualization, M.S.; methodology, M.S., P.S., A.L. and R.K.; software, not applicable; validation, E.S., V.H. and A.B.; formal analysis, M.S., K.P. and A.L.; investigation, M.S., K.P., A.L., P.S., K.O., D.G. and R.K.; resources, M.S.; data curation, M.S.; writing—original draft preparation, M.S. and A.L.; writing—review and editing, K.O. and K.P.; visualization, E.S., V.H., D.G.

and A.B.; supervision, M.S.; project administration, M.S.; funding acquisition, M.S. All authors have read and agreed to the published version of the manuscript.

Funding: This research was funded by the Director General of the Air Force Institute of Technology, Research task for 2018–2020.

Institutional Review Board Statement: Not applicable.

Informed Consent Statement: Not applicable.

Data Availability Statement: Library of Air Force Institute of Technology, Report SP-70/58/20219, ID 2698/I. According to the policy of the Air Force Institute of Technology, all the raw data supporting plots and figures are not publicly available.

Conflicts of Interest: The funders had no role in the design of the study; in the collection, analyses, or interpretation of data; in the writing of the manuscript, or in the decision to publish the results.

References

1. Chiu, W.K.; Zhou, Z.; Wang, J.; Baker, A. Battle damage repair of a helicopter composite main rotor blade. *Compos. Part B Eng.* **2012**, *43*, 739–753. [CrossRef]
2. Dobrzanski, P.; Oleksiak, W. Design and analysis methods for composite bonded joints. *Trans. Aerosp. Res.* **2021**, *1*, 45–63. [CrossRef]
3. Keegan, M.H.; Nash, D.; Stack, M. Wind Turbine Blade Leading Edge Erosion: An Investigation of Rain Droplet and Hailstone Impact Induced Damage Mechanism. Ph.D. Thesis, University of Strathclyde, Glasgow, Scotland, 2014. Available online: <https://strathprints.strath.ac.uk/58904/> (accessed on 10 January 2022).
4. Verma, A.S.; Noi, S.D.; Ren, Z.; Jiang, Z.; Teuwen, J.J.E. Minimum Leading Edge Protection Application Length to Combat Rain-Induced Erosion of Wind Turbine Blades. *Energies* **2021**, *14*, 1629. [CrossRef]
5. Herring, R.; Dyer, K.; Martin, F.; Ward, C. The increasing importance of leading edge erosion and a review of existing protection solutions. *Renew. Sustain. Energy Rev.* **2019**, *115*, 109382. [CrossRef]
6. Repairing Main Rotor Blade Leading Edge Corrosion. Available online: <https://enstromhelicopter.com/wp-content/uploads/2016/11/Repairing-Main-Rotor-Blade-Leading-Edge-Corrosion-V2.pdf> (accessed on 10 January 2022).
7. Rotor Blade Preventive Maintenance. Available online: <https://helicoptermaintenancemagazine.com/article/rotor-blade-preventive-maintenance> (accessed on 10 January 2022).
8. Sałaciński, M. Metallic helicopter blades composite repairs study case. In *Continuing Airworthiness of Aging Systems (AVT-275)*; STO/NATO: Neuilly-sur-Seine Cedex, France, 2020; pp. 247–260, ISBN 978-92-837-2255-7.
9. Sałaciński, M.; Broda, P.; Samoraj, P. *The Repair Design and Technology of Metal Rotor Blades for Mi Family Helicopters—The Approach with the Usage of Reverse Engineering*; SAE Technical Paper; SAE International: Warrendale, PA, USA, 2017. [CrossRef]
10. Stanislawski, J. Influence of Rotor Parameter Changes on Helicopter Performance and the Main Rotor Load Level. *Trans. Inst. Aviat.* **2015**, *1*, 54–69. [CrossRef]
11. Stanislawski, J. Pattern of Helicopter Rotor Loads and Blade Deformations in some states of flight envelope. *Trans. Inst. Aviat.* **2015**, *1*, 70–90. [CrossRef]
12. MON. *Remont Wirników Nośnych Śmigłowców (Lot. 1421/71)*; Ministerstwo Obrony Narodowej—Dowództwo Wojsk Lotniczych: Poznań, Polska, 1972. (In Polish)
13. Banea, M.D.; da Silva, L.F. The effect of temperature on the mechanical properties of adhesives for the automotive industry. *Proc. Inst. Mech. Eng. Part L* **2010**, *224*, 51–62. [CrossRef]
14. Gladkov, A.; Bar-Cohen, A. Parametric dependence of fatigue of electronic adhesives. In *IEEE Transactions on Components and Packaging Technologies*; IEEE: New York, NY, USA, 1999; Volume 22, pp. 200–208. [CrossRef]
15. Ashcroft, I.A.; Hughes, D.J.; Shaw, S.J.; Abdel Wahab, M.; Crocombe, A. Effect of temperature on the quasi-static strength and fatigue resistance of bonded composite double lap joints. *J. Adhes.* **2001**, *75*, 61–88. [CrossRef]
16. Raveh, A.; Zukerman, I.; Shneck, R. Thermal stability of nanostructured superhard coatings. A review. *Surf. Coat. Technol.* **2007**, *201*, 6136–6142. [CrossRef]
17. Cassidy, P.E.; Johnson, J.M.; Locke, C.E. The relationship of glass transition temperature to adhesive strength. *J. Adhes.* **1970**, *3*, 183–191. [CrossRef]
18. *Annex to ED Decision 2008/010/R*; CS-29 Certification Specifications for Large Rotorcraft CS-29; European Aviation Safety Agency: Cologne, Germany, 2008.
19. Oliver, J.E. Standard atmosphere. In *Climatology. Encyclopedia of Earth Science*; Springer: Boston, MA, USA, 1987. [CrossRef]
20. Gebura, A.; Poradowski, M. Thermovision and electricity capacitance measurements as an evaluation of a helicopter rotor blades delamination. *J. Konbin* **2015**, *4*, 187–200. [CrossRef]
21. Sałaciński, M.; Zabłocka, M.; Synaszko, P. Using sandblasting and sol gel techniques for the preparation of a metal surface and their effects on the durability of epoxy-bonded joints. *Fatigue Aircr. Struct.* **2012**, *1*, 94–99. [CrossRef]

22. Panas, A.J.; Białecki, M.; Dudziński, A.; Figur, K.; Krupińska, A.; Nowakowski, M.; Omen, Ł. Badania właściwości cieplnofizycznych i cieplnomechanicznych lotniczego kompozytu epoksydowo-szklanego. In *Mechanika w Lotnictwie*; Polskie Towarzystwo Mechaniki Teoretycznej i Stosowanej: Warszawa, Polska, 2018; Volume II, pp. 163–172. (In Polish)
23. Panas, A.J. Wysokorozdzielcze termodynamiczne badania rozszerzalności liniowej dylatometryczna analiza termiczna. In *Rozprawa Habilitacyjna*; Wojskowa Akademia Techniczna: Warszawa, Polska, 1998. (In Polish)
24. Kinloch, A.J. *Durability of Structural Adhesives*; Springer: Amsterdam, The Netherlands, 1983; ISBN 978-0-85334-214-4.
25. Molitor, P.; Barron, V.; Young, T. Surface treatment of titanium for adhesive bonding to polymer composites: A review. *Int. J. Adhes. Adhes.* **2001**, *2*, 129–136. [[CrossRef](#)]
26. Ramani, K.; Weidner, W.G.; Kumar, G. Silicon sputtering as a surface treatment to titanium alloy for bonding with PEKEKK. *Int. J. Adhes. Adhes.* **1998**, *6*, 401–412. [[CrossRef](#)]
27. Blohowiak, K.Y.; Grob, J.W.; Seebergh, J.E. AVTIP—Air Vehicle Technology Integration Program; AFRL-ML-WP-TR-2006-4042 Final Report; The Boeing Company: Chicago, IL, USA, 2005.
28. Filbey, J.A.; Wightman, J.P. Factors Affecting the Durability of Titanium/Epoxy Bonds. In *Adhesion 12*; Allen, K.W., Ed.; Springer: Dordrecht, The Netherlands, 1988. [[CrossRef](#)]
29. Kohli, R. Methods for Monitoring and Measuring Cleanliness of Surfaces. In *Developments in Surface Contamination and Cleaning*; Elsevier: Waltham, MA, USA, 2012; pp. 107–178. [[CrossRef](#)]
30. Ellis, B. The water break test. *Circuit World* **2005**, *31*, 47. [[CrossRef](#)]
31. ASTM F22-02; Standard Test Method for Hydrophobic Surface Films by the Water-Break Test. ASTM International: West Conshohocken, PA, USA, 2007.
32. Rafil—Data Sheet, Radomska Fabryka Farb i Lakierów Polska. 2021. Available online: https://www.rafil.pl/wp-content/uploads/2018/05/KTW_09_04-2.pdf (accessed on 11 January 2022). (In Polish)
33. Cytec. BR®127 Corrosion Inhibiting Primer Cytec Engineering Materials. 2010. Available online: <https://www.cytec.com> (accessed on 14 January 2022).
34. Scotch-Weld EPX Adhesive DP490—Data Sheet, 3M Company. 1996. Available online: https://www.van-asperen.nl/userdata/file/3M_DP490_Datasheet.pdf (accessed on 11 January 2022).
35. Scotch-Weld Epoxy Adhesive 2216 B/A—Data Sheet, 3M Company. 2018. Available online: <https://multimedia.3m.com/mws/media/153955O/3mtm-scotch-weldtm-epoxy-adhesive-2216-b-a.pdf> (accessed on 11 January 2022).
36. Kaczorowska, E. Dobór procesu kondycjonowania próbek zgodnie z wymaganiami kwalifikacji kompozytów polimerowych do zastosowań w konstrukcjach lotniczych. *Pr. Inst. Lotnictwa* **2016**, *3*, 83–89. (In Polish) [[CrossRef](#)]
37. Niu, M.; Niu, C.Y. *Composite Airframe Structures*; Hong Kong Conmilit Press Ltd.: Hong Kong, China, 1998; ISBN 9627128066.
38. Peters, S.T. *Handbook of Composites*; Chapman & Hall: London, UK, 1998; ISBN 978-0-412-54020-2.
39. Szumiak, J.; Smoczyński, Z.; Szcześniak, K. Armament and military equipment polymer composite ageing. *Sci. J. Mil. Univ. Land Forces* **2011**, *1*, 273–285. Available online: <https://yadda.icm.edu.pl/baztech/element/bwmeta1.element/baztech-article-BATA-0010-0024> (accessed on 11 January 2022).
40. European Aviation Safety Agency. Type Certificate Data Sheet No. EASA.R.509 for AW169 Type Certificate Holder Leonardo, S.p.A, 2022. Available online: <https://www.easa.europa.eu/downloads/18869/en> (accessed on 11 January 2022).
41. European Aviation Safety Agency. Type Certificate Data Sheet No. EASA.A.004 for AIRBUS A330 Type Certificate Holder AIRBUS. 2020. Available online: <https://www.easa.europa.eu/sites/default/files/dfu/A330%20EASA%20TCDS%20A.004%20-%20Issue%2056.pdf> (accessed on 23 June 2021).
42. European Aviation Safety Agency. Type Certificate Data Sheet No. EASA.R.150 for EC 175 Type Certificate Holder Airbus Helicopters. 2022. Available online: <https://www.easa.europa.eu/downloads/16512/en> (accessed on 11 January 2022).
43. European Aviation Safety Agency. Type Certificate Data Sheet No. EASA.R.105 for SA 365/AS 365/EC 155 Type Certificate Holder Airbus Helicopters, 2021. Available online: <https://www.easa.europa.eu/downloads/16527/en> (accessed on 11 January 2022).
44. European Aviation Safety Agency. Type Certificate Data Sheet No. EASA.R.508 for EC 120 Type Certificate Holder Airbus Helicopters. 2019. Available online: <https://www.easa.europa.eu/downloads/7911/en> (accessed on 23 June 2021).
45. European Aviation Safety Agency. Type Certificate Data Sheet No. EASA.A.444 for PZL-106 BT Turbo Kruk Series Type Certificate Holder Airbus Poland, S.A. 2019. Available online: https://www.easa.europa.eu/sites/default/files/dfu/TCDS_EASA.A.444_PZL-106BT_Turbo_Kruk_iss-02.pdf (accessed on 23 June 2021).
46. NO-06-A103 2005; Uzbrojenie i Sprzęt Wojskowy—Ogólne Wymagania Techniczne, Metody Kontroli i Badań—Wymagania Środowiskowe. Ministerstwo Obrony Narodowej: Warszawa, Polska, 2005. (In Polish)
47. The United States Department of Defense. Composite Materials Handbook Vol. 1—Polymer Matrix Composites Guidelines for Characterization of Structural Materials; MIL-HNDB-17-1F; 2002. Available online: http://everyspec.com/MIL-HDBK/MIL-HDBK-0001-0099/MIL_HDBK_17_1F_237/ (accessed on 15 May 2021).
48. Standard Temperature Variation at Different Altitudes. Available online: <https://www.ambrsoft.com/CalcPhysics/Altitude/altitude.htm> (accessed on 6 June 2020).
49. Samroff, A.M.; Frost, P.D. *The Hot Extrusion of Titanium and Titanium Alloys*; Report No. 53; Titanium Metallurgical Laboratory, Battle Memorial Institute: Columbus, OH, USA, 1956.
50. ASTM D1002-10; Standard Test Method for Apparent Shear Strength of Single-Lap-Joint Adhesively Bonded Metal Specimens by Tension Loading (Metal-to-Metal). ASTM International: West Conshohocken, PA, USA, 2019.

51. Bamford, C.H.; Tipper, C.F.H. Degradation of Polymers. In *Comprehensive Chemical Kinetics*; Elsevier: Amsterdam, The Netherlands, 1975; Volume 14.
52. Kockott, D. *Factors Influencing the Reliability of Results in Accelerated Weathering Tests*; ASTM Special Technical Publication STP: West Conshohocken, PA, USA, 1996; Volume 1294.
53. Wypych, G. *Handbook of Material Weathering*; Chemtec Publishing: Netanya, Israel, 2007.
54. Rojek, M. *Metodologia Badań Diagnostycznych Warstwowych Materiałów Kompozytowych o Osnowie Polimerowej*; Open Access Library: Gliwice, Polska, 2011; Volume 2, pp. 1–148. (In Polish)
55. Mohd Aris, K.D.; Shariff, M.F.; Abd Latif, B.R.; Mohd Haris, M.Y.; Baidzawi, I.J. A comparison of damage profiling of automated tap testers on aircraft CFRP panel. *AIP Conf. Proc.* **2017**, *1901*, 130009. [[CrossRef](#)]
56. Hsu, D.K. Nondestructive inspection of composite structures: Methods and practice. In Proceedings of the 17th World Conference on Nondestructive Testing, Shanghai, China, 25–28 June 2008. Available online: <https://www.ndt.net/article/wcndt2008/papers/612.pdf> (accessed on 11 February 2021).